Optimum Bias Conditions for Linear Broadband InGaP/GaAs HBT Power Amplifiers

Masaya Iwamoto, Craig P. Hutchinson*, Jonathan B. Scott*, Thomas S. Low*,
Mani Vaidyanathan, Peter M. Asbeck, and Don C. D'Avanzo*

Dept. of Electrical and Computer Engineering, Univ. of California at San Diego, La Jolla, CA
*Microwave Technology Center, Agilent Technologies, Santa Rosa, CA

Abstract — **A design strategy for a linear broadband InGaP/GaAs HBT power amplifier is presented. This design takes advantage of the bias dependence of the nonlinear base-collector charge, expressed by the C_{BC} vs V_{CE} and τ_C vs I_C characteristics of the device. Using this technique, it is shown that the second and third order distortions have separate optimum bias conditions, and furthermore, there is an inherent tradeoff in optimizing the second and third order distortions. This strong bias dependence of the nonlinear base-collector charge and the tradeoff between the different orders of distortion are verified on a 24dBm 0.5-11GHz distributed power amplifier. To minimize high frequency distortion in HBT amplifiers across a wide range of bias, it is imperative to linearize the base-collector charge, where flat C_{BC} vs V_{CE} and f_t vs I_C characteristics are ideally desired.**

I. Introduction

Wide bandwidth power amplifiers are essential in such applications as broadband test instrumentation (i.e. signal sources) and cable television distribution. Typically in these applications, high bandwidth and linearity are critical specifications, and efficiency is a less important requirement. One of the challenges in designing broadband power amplifiers is to maintain high linearity over the entire bandwidth, since narrowband linearization techniques cannot be utilized. In this paper, we present an intuitive design methodology for an InGaP/GaAs HBT broadband power amplifier, which achieves high linearity over a wide range of frequencies based on properly identifying linear bias points from s-parameter data. More specifically, the optimum bias points are chosen by observing the nonlinear behavior of the base-collector capacitance (C_{BC}) with collector-emitter voltage and of the unity current gain frequency (f_t) with collector current.

II. Bias Dependence of Distortion in HBTs

Experimental and analytical studies of weak nonlinearities in GaAs HBTs have shed light on several sources of distortion. The most apparent source of distortion is due to the exponential relationship between input voltage and the output current, quantified by the

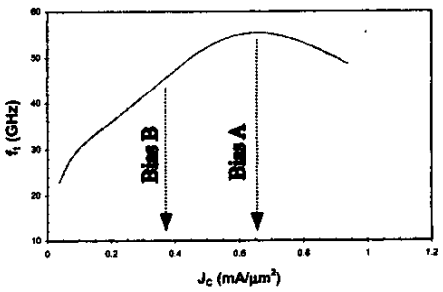

1a)

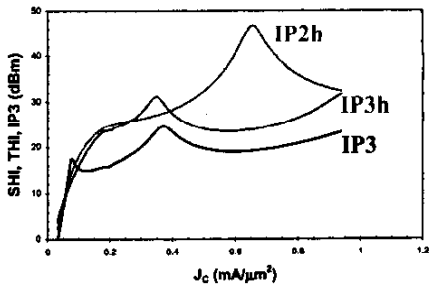

1b)

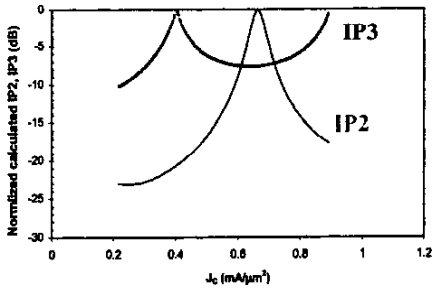

1c)

Fig. 1 a) f_t vs J_C of a discrete HBT device at V_{CE}=4V.
b) Second harmonic intercept (IP2h), third harmonic intercept (IP3h), and third order intercept point (IP3) at 5GHz.
c) Normalized plot of equations (1) and (2).

0-7803-7239-5/02/$10.00 © 2002 IEEE

transconductance (g_m). This g_m nonlinearity is dominant at low bias currents and is inherently linearized by the base and emitter resistances at high currents [1]. Another identified source of distortion is the nonlinear behavior of C_{BC} with bias [2]. Experimental studies have shown improved linearity by biasing the collector voltage high to fully deplete the collector, which results in an approximately constant C_{BC}. In addition, it has been experimentally shown that the nonlinearity due to the base-collector transit time ($\tau_{BC}=\tau_B+\tau_C$) is a significant source of distortion at high currents [3]. This nonlinearity can be observed by plotting f_t vs. J_C and distortion vs. J_C as shown in Figs. 1a and 1b. τ_B and τ_C are related to f_t since $1/(2\pi f_t)$ represents the total delay between the emitter and collector. τ_B represents the delay associated with the minority carrier transport across the base region, including the current induced base region due to Kirk effect. τ_C represents the delay associated with electrons traversing the collector depletion region. At high current densities below the onset of Kirk effect, the nonlinear behavior of f_t is predominantly influenced by τ_C due to the complex variation of electron velocity with the electric field profile in the collector depletion region. τ_B, on the other hand, does not become significantly nonlinear until base-pushout occurs above the Kirk effect threshold current. It is interesting to note that C_{BC} and τ_C are related to each other, since C_{BC} and τ_C are derivatives of the base-collector charge (Q_{BC}) with respect to V_{BC} and I_C, respectively. Therefore, it can be said that the nonlinearities due to C_{BC} and τ_C are tied to a single non-linear source, Q_{BC}. It is also interesting that the nonlinear behavior of electron velocity with electric field of the GaAs collector (due to inter-valley transfer of electrons in the conduction band) directly influences the distortion characteristics of GaAs HBTs.

The results of Fig. 1b can be elucidated by quantifying the relationship between f_t and distortion. Using a simple small-signal model and assuming that the nonlinear relation between Q_{BC} and I_C (as implied by the f_t vs I_C relation) is the dominant source of nonlinearity, it can be shown that the linearity figures of merit IP2 and IP3 are related to f_t by,

$$\frac{1}{IP2} \sim \left(\frac{1}{f_t} \frac{\partial f_t}{\partial I_C} \right)^2 \quad (1)$$

$$\frac{1}{IP3} \sim \left(\frac{1}{f_t} \frac{\partial f_t}{\partial I_C} \right)^2 + \frac{1}{2 f_t} \frac{\partial^2 f_t}{\partial I_C^{\,2}} \quad (2)$$

Plots of these quantities based on data from Fig. 1a are shown in Fig. 1c (with arbitrary constants of proportionality). Agreement between the shapes of the corresponding curves is striking. It should be stressed that Fig. 1c was simply constructed by performing a polynomial fit to the f_t vs J_C characteristics of Fig 1a and then applying (1) and (2).

(1) states that to minimize second order distortion due to transit time, the device should be biased at a current where the slope of f_t vs. J_C is at a minimum and the magnitude of f_t is at a maximum. Fortunately, these two conditions are simultaneously met at the f_t peak. This relationship is clearly evident in Fig. 1 and has also been experimentally observed in Si BJTs [4].

According to (2), the third order distortion due to transit time is more complex since both the slope and curvature of f_t are involved. It can be seen from Figs. 1b and 1c that any significant curvature in the f_t vs J_C characteristics is detrimental to third order distortion. The peak in IP3 occurs where the curvature is small and a local minimum in IP3 exists where the curvature is at a maximum (at peak f_t). Since the slope and curvature cannot be typically minimized simultaneously (unless the f_t behavior of the device is designed to be flat), there is a tradeoff in optimizing second and third order distortions. A more detailed analysis of high frequency distortion in HBTs will be presented in [5].

III. Design Strategy for Optimized Distortion

A 24dBm four-stage distributed power amplifier optimized for second order distortion was designed with a decade of bandwidth. To minimize the distortion from C_{BC}, V_{CE} is set high to fully deplete the collector. This condition is easily met in this design, since V_{CE} has to be set high as possible to maximize output power. Also, the bias current is selected by considering the maximum power and load line for Class A operation. Determining the current *density* bias is the critical design point to achieve high linearity. As mentioned in the previous section, to minimize the second harmonic distortion, the current density should be set where the f_t peaks (at Bias A). This is done by properly scaling the areas of each cell.

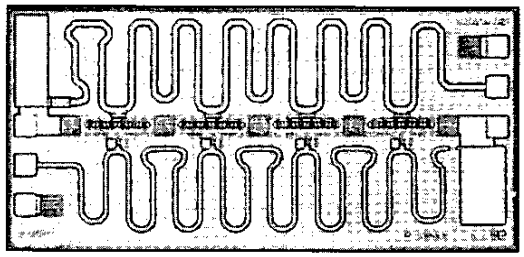

Fig. 2: Photograph of the HBT distributed power amplifier MMIC optimized for second harmonic distortion

After the bias point is selected, the input and output matching is done using standard distributed amplifier design methodology. A major design issue for HBT distributed amplifiers is that the diffusion capacitance dominates the effective input capacitance [6]. This limits the bandwidth of the amplifier and is further exacerbated for power amplifiers since the diffusion capacitance is proportional to the bias current. To alleviate this problem, a coupling capacitor is placed in series with the input to reduce the effective input capacitance at the cost of gain [7]. Emitter resistor ballasting further reduces diffusion capacitance, though its main purpose is for thermal management. To simplify the testing, the biasing of the input and output is achieved through bias tees. A photograph of the completed MMIC circuit is shown in Fig 2.

IV. Measurement Results

The frequency response of the amplifier was evaluated using the Agilent 8510C network analyzer. Although the amplifier was optimally designed for low second harmonic distortion (Bias A), it can also be biased at the optimal third order distortion point (Bias B) by reducing the current to the appropriate value. Fig. 3 shows the s-parameters measured at the two bias points. It is evident that the s-parameters for the two biases look very similar although the bias current densities are different. This is attributed to the fact that the input and output impedances of each stage are predominantly determined by the value of the coupling capacitor and the emitter ballasting resistors. The gain is 7.5±1dB with 0.5-11GHz bandwidth. Good input and output matches are also obtained within this bandwidth.

Harmonic distortion measurements were made at the two bias points. Fig 4a shows a single tone power sweep at

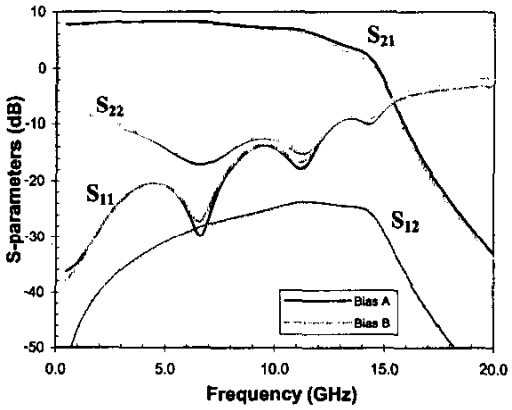

Fig. 3: S-parameters measured at Bias A and Bias B

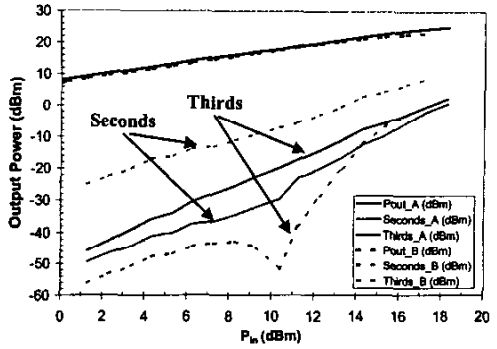

4a)

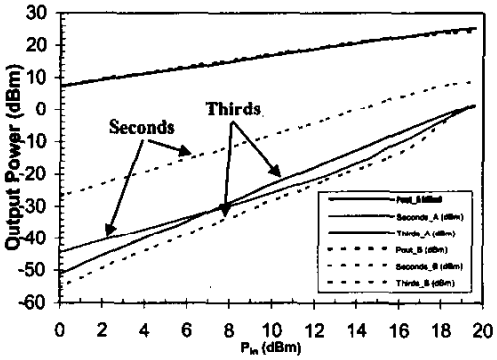

4b)

Fig. 4: Second and third harmonic distortion at Bias A and Bias B: a)1GHz and b)5GHz

1GHz and Fig 4b shows a similar measurement at 5GHz. At 1GHz, P_{1dB} is at 25dBm for Bias A and 23dBm for Bias B. Although the two bias points have similar gain, it is evident that the second and third harmonic distortion components are strikingly different. For Bias A, the second harmonic distortion component is low while the third harmonic distortion power is relatively high. Since each cell is biased at the f_t peak, this behavior is consistent with the characteristics observed in Fig. 1. For Bias B, the converse of what is observed for harmonic distortion in Bias A occurs. Relative to Bias A, the second harmonic distortion worsens due to an increase in the slope of f_t vs. J_C and the third harmonic distortion improves due to a decrease in the curvature of f_t vs. J_C. It can be observed that the improvement or degradation in distortion power is very significant between the two bias points. Also, this biasing technique is effective for a wide range of output power. Similar trends are observed at 5GHz as seen in Fig 4b. At this frequency, P_{1dB} of the amplifier is 24dBm for Bias A and 22dBm for Bias B.

To further understand the effectiveness of this broadband design approach, harmonic and intermodulation distortions were measured at small-signal power over frequency. Fig. 5a shows second harmonic intercept (IP2h), third harmonic intercept (IP3h), and third order (intermodulation) intercept point (IP3). The tradeoffs in optimizing the second and third order distortions are again evident between the two bias points. It can be seen that this tradeoff is consistent over a wide range of frequencies. Fig. 5b shows second and third harmonic distortions measured at a fixed fundamental power of 20dBm over frequency. This fundamental output power level is large-signal since it is only several dBs backed-off from P_{1dB}. Similar trends are observed between the two bias points and over frequency. In general, to optimize both second and third harmonic distortions, the optimum bias point lies somewhere between Bias A and Bias B. From the view of the device, it is desirable to bias the current just below the peak of the f_t vs. J_C curve.

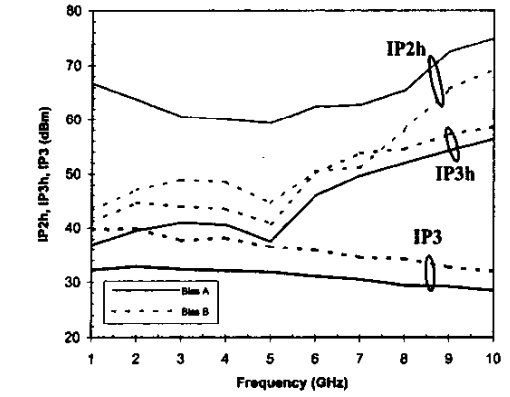

5a)

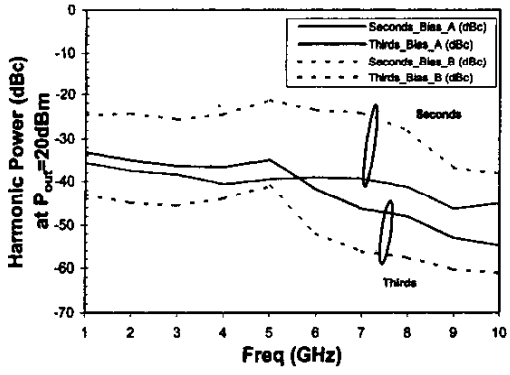

5b)

Fig. 5 a) IP2h, IP3h, IP3 vs. frequency at Bias A and Bias B
b) Second harmonic and third harmonic powers vs. frequency measured at 20dBm fixed fundamental output power

V. Conclusion

A design approach for a linear broadband power amplifier was presented. The circuit is based on the distributed amplifier topology and optimum linearity is achieved through careful observation of the nonlinear bias dependence of the base-collector charge. With this biasing method, there is an inherent tradeoff in optimizing the second and third order distortion components. Measurements indicate that this biasing technique is applicable over a wide range of frequencies. Ultamately, to minimize the high frequency distortion in HBTs, the bias dependence of C_{BC} and f_t should be minimized.

Acknowledgement

The authors appreciate the valuable assistance from the following people at Agilent Technologies, Santa Rosa, CA: Jerry Orr, Christian Bourde, and Dan Scherrer (for discussions on circuit design); Denise Davis and Vi Moir (for layout issues); and John Wood and Xiaohui Qin (for passive model definitions). They also greatly appreciate the support and encouragement from David Root, Brian Hughes, Tim Shirley, Derry Hornbuckle, and Jerry Gladstone of Agilent Technologies.

References

[1] N.L. Wang, W.J. Ho, J.A. Higgins, "AlGaAs/GaAs HBT Linearity Characteristics", *IEEE Trans. Microwave Theory and Techniques*, vol 42, no. 10, pp1845-1850, Oct. 1994.

[2] W. Kim, S. Kang, K. Lee, M. Chung, Y. Yang, and B. Kim, "The Effects of C_{BC} on the Linearity of AlGaAs/GaAs Power HBTs", *IEEE Trans. Microwave Theory and Technique*, vol. 49, pp. 1270-1276, July 2001.

[3] M. Iwamoto, T.S. Low, C.P. Hutchinson, J.B. Scott, A. Cognata, X. Qin, L.H. Camnitz, P.M. Asbeck, D.C. D'Avanzo, "Linearity Characteristics of InGaP/GaAs HBTs and the Influence of Collector Design," *IEEE Trans. Microwave Theory and Technique*, vol. 45, pp. 2377-2388, Dec 2000.

[4] M. Schröter, D. Pehlke, T.-Y. Lee, "Compact Modeling of High-Frequency Distortion in Silicon Integrated Bipolar Transistors," *IEEE Trans. On Electron Devices*, vol. 47, no. 7, pp1529-1535, July 2000.

[5] M. Vaidyanathan, M. Iwamoto, L.E. Larson, P.S. Gudam, P.M. Asbeck, "A Basic Theory of High-Frequency Distortion in Bipolar Transistors," *submitted to IEEE Transactions on Microwave Theory and Techniques*

[6] J.P. Viaud, M. Lajugie, R. Quéré, J. Obregon, "First Demonstration of a 0.5W, 2 to 8GHz MMIC HBT Distributed Power Amplifier Based on a Large Signal Design Approach," *IEEE International Microwave Symposium*, p893-896, June 1997.

[7] Y. Ayasli, S.W. Miller, R. Mozzi, L.K. Hanes, "Capacitively Coupled Traveling-wave Power Amplifier," *IEEE Transactions on Electron Devices*, vol. 31, pp1937-1942, Dec. 1984.